Self-Assembled DNA Immunonanoflowers as Multivalent CpG Nanoagents

Liqin Zhang,[†,§] Guizhi Zhu,[†,‡,§] Lei Mei,[‡] Cuichen Wu,[†,‡] Liping Qiu,[‡] Cheng Cui,[†] Yuan Liu,[†] I-Ting Teng,[†] and Weihong Tan*[,†,‡]

[†]Departments of Chemistry, Physiology and Functional Genomics, Center for Research at the Bio/Nano Interface, UF Health Cancer Center, UF Genetics Institute and McKnight Brain Institute, University of Florida, Gainesville, Florida 32611, United States

[‡]Molecular Science and Biomedicine Laboratory, State Key Laboratory of Chemo/Bio-Sensing and Chemometrics, College of Chemistry and Chemical Engineering, College of Biology, Collaborative Innovation Center for Chemistry and Molecular Medicine, Hunan University, Changsha 410082, China

Ⓢ Supporting Information

ABSTRACT: Synthetic unmethylated cytosine—guanine (CpG) oligodeoxynucleotides are immunostimulatory motifs that have shown promise as vaccines or adjuvants for diseases such as cancers and infectious diseases. In the present work, novel immuno-nanoflowers (NFs), self-assembled from long DNA integrated with tandem CpG through rolling circle replication, were developed for efficient CpG delivery and protection from nuclease degradation. In a model of macrophage-like cells, the CpG NFs proved to be potent immunostimulators by triggering the proliferation of these immune cells, which, in turn, secreted immunostimulatory cytokines, including tumor necrosis factor α, interleukin-6, and interleukin-10. These results demonstrate the ability of CpG NFs to induce cancer cell apoptosis and necrosis.

KEYWORDS: DNA, immunonanoflower, CpG ODNs, immunostimulation, nanoagent
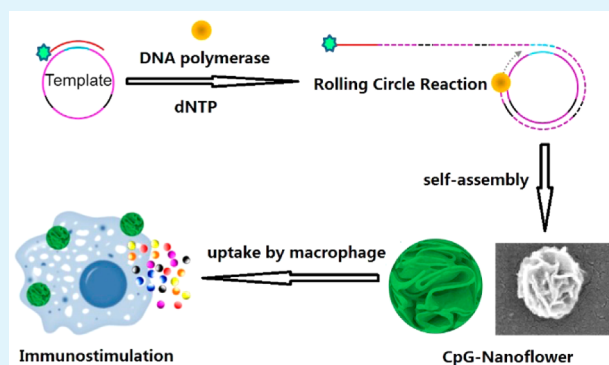
1. INTRODUCTION

Immunotherapy seeks to exploit the host immune system for disease prevention and therapy.[1] Approaches range from engineered immune cells, such as T cells, dendritic cells, or macrophages, to immunostimulatory molecules or molecular complexes, such as vaccines and immunoregulatory cytokines.[2−6] Among these approaches, immunostimulatory nucleic acids, mainly including cytosine—guanine (CpG) DNA motifs[5] and polyinosinic:poly(cytidylic acid) (poly-I:C) RNA motifs,[7] are emerging as promising safe, yet effective, regimes to boost the immune system and combat diseases. Unmethylated CpG DNA motifs are derived from bacterial or viral genomes, such as pathogen-associated molecular patterns (PAMPs). These CpG motifs can be specifically recognized by Toll-like receptor 9 (TLR9), a transmembrane pattern recognition receptor found mainly on the cell endosomes in many immune cells, including dendritic cells, NK, macrophages, monocytes, or B cells.[8,9] Once TLR9 has recognized PAMPs expressed by infectious pathogens, or in this case CpG motifs, TLR9 changes its conformation to recruit adapter protein MyD88, in turn triggering activation of the transcription factor nuclear factor kappaB and the phosphorylation of mitogen-activated protein kinase.[10,11] This initiates the expression of proinflammatory cytokines, including tumor necrosis factor α (TNF-α), interleukin-6 (IL-6), and interleukin-10 (IL-10), thereby inducing innate and adaptive immune responses.[10] Because of their similar immunostimulatory capacity, synthetic CpG oligodeoxynucleotides (ODNs) have been intensively studied as vaccines or vaccine adjuvants for the treatment of various diseases, ranging from cancers, allergies, and asthma to infectious diseases.[9−11]

However, the successful delivery of synthetic CpG ODNs into immune cells faces several challenges. First, negatively charged CpG ODNs are not efficiently uptaken by immune cells. Second, CpG ODNs are susceptible to nuclease degradation, resulting in a short half-life under physiological conditions.[12] Under these conditions, target cells cannot be reached as a result of the relatively small molecular weight of CpG ODNs. To address these challenges, current approaches include chemical modifications of CpG ODNs with a phosphorothioate backbone,[13] lipids,[14−16] G-rich DNA ligands,[17] and nanotechnologies, such as gold nanoparticles,[18−20] DNA tetrahedra,[21] and DNA hydrogels.[22] However, each of these approaches requires complex chemical modification, use of nonnatural material as vehicle, or relatively complicated DNA nanostructure design and assembly. In addition, there are

safety concerns over the use of nonnatural materials and double-stranded DNA (dsDNA), which may induce anti-dsDNA antibodies and trigger an autoimmune response.[23]

As an alternative, we have taken advantage of our recently developed multifunctional DNA nanoflowers (NFs)[24,25] for CpG ODN delivery. To accomplish this, DNA NFs were first self-assembled from elongated DNA building blocks generated through rolling circle replication (RCR). It is worth noting that NF assembly does not rely on Watson–Crick base pairing, thus removing the potential safety concern of dsDNA, which is ubiquitous in conventional DNA nanostructures assembled by hybridization. Composed of DNA molecules and likely magnesium pyrophosphate produced in the polymerization process,[26] these biocompatible NFs are resistant to nuclease degradation or denaturation at high temperature or at low concentration (100-fold dilution).[24] Given their size scale (100–300 nm), NFs can be easily taken up by macrophages, which are scavenger cells that engulf cell debris or any foreign materials and are professional antigen-presenting cells.[27] Most importantly, NFs are inherently ready for functionalization with molecular recognition ligands and imaging agents.[25] All of these properties make NFs a perfect tool for CpG intracellular delivery. Here we report the first example of the incorporation of CpG ODN, as a model nucleic acid therapeutic, into NFs, which served as both structural vehicles for therapeutics and stand-alone therapeutics, for efficient CpG delivery and potent immunostimulation (Figure 1).
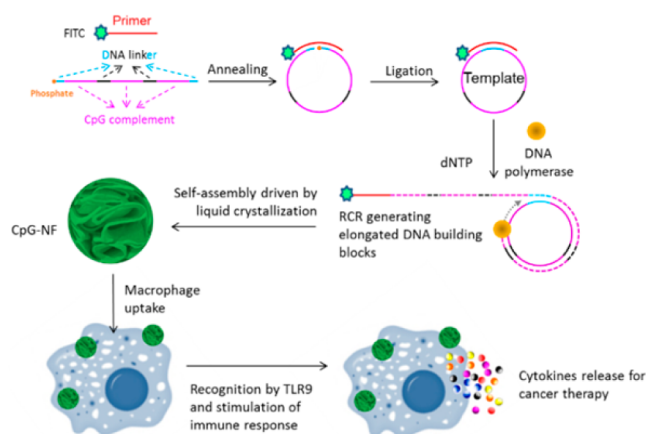

Figure 1. Schematic illustration of self-assembled DNA immuno-NFs for immunostimulation. The linear DNA templates composed of CpG complements and linkers and FITC-labeled primers were first annealed and ligated to form a circular template. RCR was performed by using Φ29 DNA polymerase to generate a large amount of elongated nonnicked concatemer DNA with each unit complementary to the template. NFs were then self-assembled via liquid crystallization. After being uptaken by macrophages, these NFs could be recognized by TLR9, followed by the secretion of cytokines.

2. RESULTS AND DISCUSSION

CpG 1826[14] was chosen as a model CpG ODN in this study. For RCR, a linear template was designed to contain three copies of complementary CpG (Table S1) and phosphorylated at the 5′ end. The template was circularized by ligation of the annealed template primer using T4 DNA ligase, followed by RCR using Φ29 DNA polymerase, which was confirmed using agarose gel electrophoresis (Figure S1). The resultant mixture was inactivated by heating at 65 °C, washed, and centrifuged for
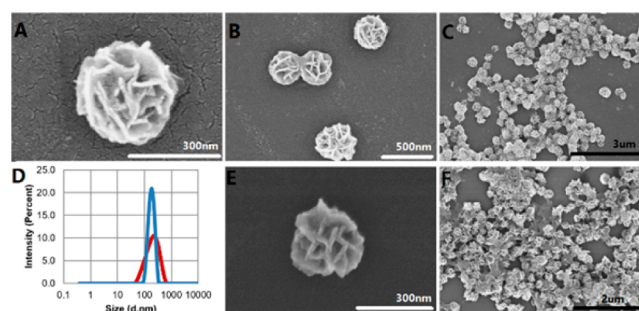

Figure 2. Structural characterization of nuclease-resistant NFs. (A–C) SEM images showing structures of NFs at different scales. (D) DLS size distribution of NFs before (red) and after (blue) treatment with 5 U/mL of DNase I for 24 h at 37 °C. (E and F) SEM images showing structures of NFs after treatment with 5 U/mL of DNase I for 24 h at 37 °C.
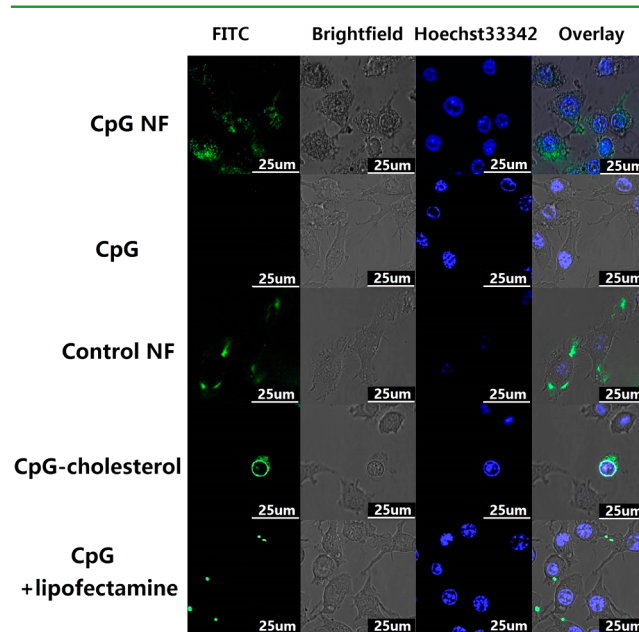

Figure 3. Confocal images showing the internalization of NFs by RAW264.7 macrophages. Confocal microscopy images showing that CpG NFs (100 nM CpG equivalents), as well as control NFs, were internalized into RAW 264.7 macrophages after incubation for 2 h. NFs were incorporated with FITC (green) by attaching it to the 5′ end of the RCR primer. 3′-end-FITC-labeled CpG ODNs were used as a negative control group. Internalization of FITC–CpG–cholesterol conjugation and lipofectamine-mediated CpG FITC was also investigated and compared.

purification. With 6 h of RCR, monodisperse NFs were assembled having an average diameter of approximately 300 nm, as determined by both scanning electron microscopy (SEM) observation (Figure 2A–C) and dynamic light scattering (DLS) analysis (Figure 2D). SEM images also confirmed the monodispersity of NFs, which displayed petal-shaped structures on their surfaces. Furthermore, NFs treated with DNase I displayed size distribution and morphology comparable to those of intact NFs (Figure 2D–F), which is consistent with our previous reports about the resistance of CpG NFs to nuclease degradation.[24,25] This may be attributed to the dense packaging of DNA in NFs, which prevents direct contact between nuclease and the inner layer of DNA molecules and retards the digestion process to a great extent.
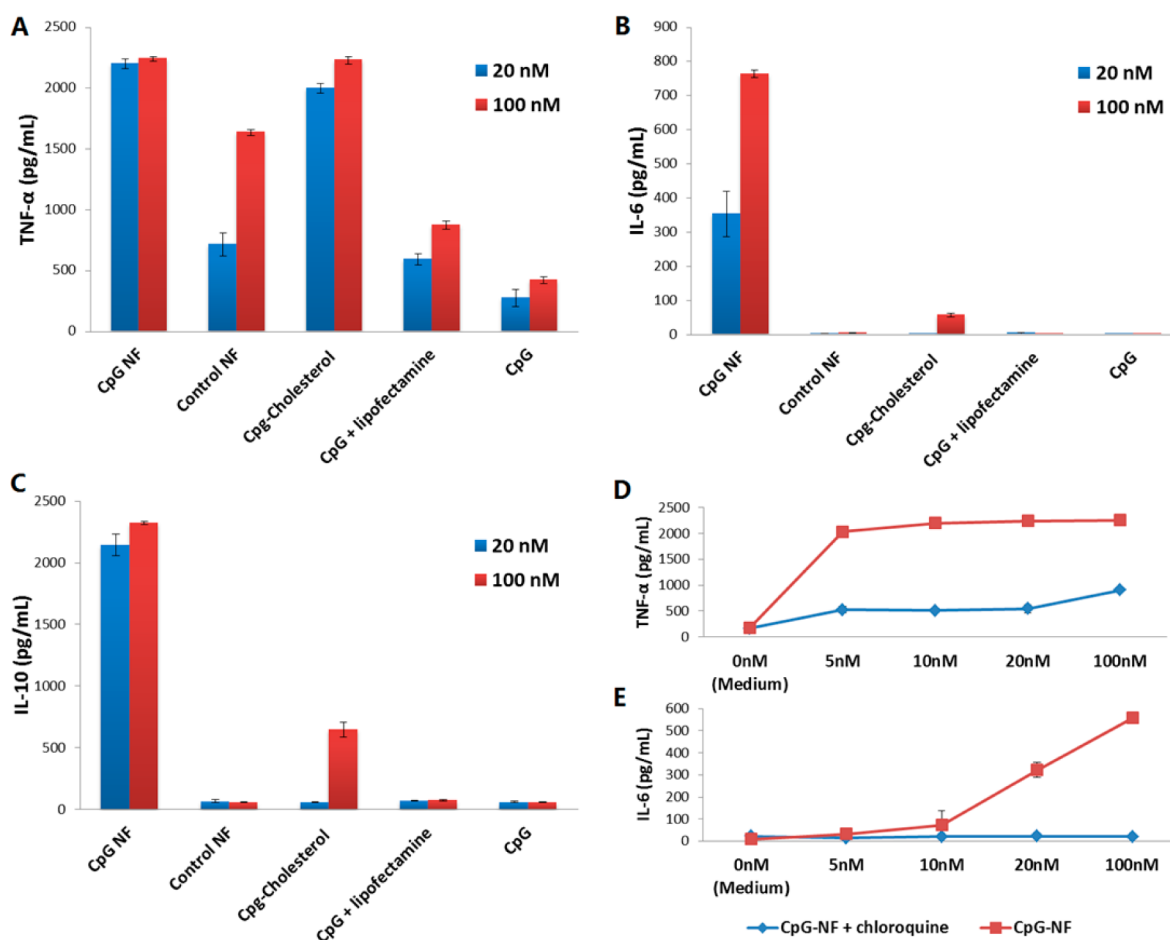
Figure 4. Secretion of cytokine stimulated by CpG NFs. CpG NFs induce potent immunostimulation, as demonstrated by significantly elevated immunocytokines induced by CpG NFs in ELISA assay. (A−C) ELISA assay results of cytokine secretion stimulated by CpG NFs and other control groups. (D and E) ELISA assay results of cytokine secretion stimulated by different concentrations of CpG NFs with/without treatment with chloroquine.

Next we evaluated the biocompatibility of CpG NFs in a living system. As a model, mouse macrophage RAW264.7 cells were used in this study. We first performed an MTS assay using CpG NFs in this cell line to (1) confirm the biocompatibility at the cellular level and (2) evaluate the potential impact of CpG NFs on the stimulation of immune cell proliferation and activation, an essential part of immunostimulation. To accomplish these aims, CpG NFs were incubated with RAW264.7 cells for 24 h prior to MTS assay. The concentration of CpG NFs was measured based on the number of CpG copies involved in all NFs in the treatment group. The control CpG contained the same number of DNA copies with CpG NF groups in the same volume of solvent but with random sequences. The results (Figure S2) clearly showed that (1) CpG NFs did not inhibit cell proliferation and are, therefore, biocompatible under our experimental conditions and (2) proliferation of these immune cells was specifically stimulated by CpG NFs, as indicated by the enhanced cell viability, but not significantly observed in control NF groups. Stimulation of the proliferation of immune cells by CpG motif-mediated activation of TLR9 is consistent with previous findings.[21]

For optimal delivery of CpG ODNs to stimulate immune cell response, the ODNs have to be internalized into cells, particularly to reach endosomes, where TLR9 is primarily expressed. The nanoscale size of NFs should be a favorable factor for easy capture by macrophages, resulting in de facto internalization. To confirm this assumption, CpG NFs, as well as control NFs with a nonsense sequence, were labeled with FITC by attaching FITC on the 5′ end of the DNA primer used to initiate RCR. RAW 264.7 cells were allowed to grow for 24 h prior to incubation with 100 nM CpG NFs for 2 h. Hoechst 33342 was used to identify the nucleus. As observed under confocal microscopy (Figures 3 and S3), FITC fluorescence was distributed in the cytoplasm, verifying that CpG NFs were internalized in the cytoplasm of these macrophages, whereas 3′-end-FITC-labeled CpG ODNs showed a minimum level of internalization.

NFs were then evaluated for their therapeutic efficacy, particularly their ability to simulate immune cells. One of the biological consequences of immune cell stimulation is the secretion of immune cytokines. Particularly for CpG ODNs, immune cells can secrete a variety of immune regulators, including TNF-α, IL-6, and IL-10. Combining the characteristic properties of high loading capacity, resistance to nuclease degradation or denaturation, and capacity for efficient internalization, CpG NFs were expected to be potent immunostimulators able to induce the secretion of large amounts of cytokines. To test this, RAW264.7 macrophages were treated with CpG NFs, in a fresh medium, for a defined time period, along with those treated with free CpG ODNs and control NFs. To compare the immunostimulation potency of CpG NFs
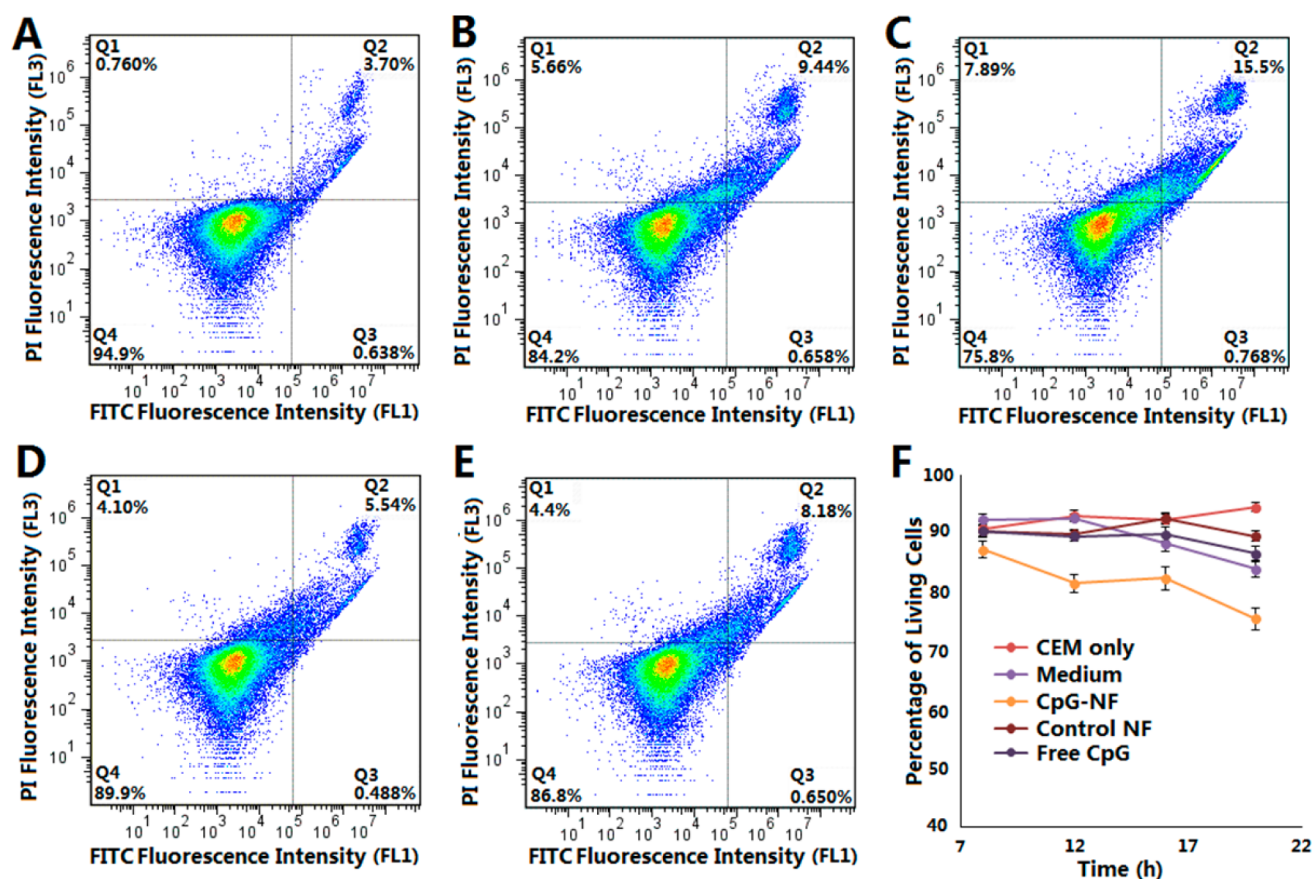
Figure 5. Preliminary in vitro evaluation of the therapeutic effect of immunostimulatory CpG NFs on cancer cells. Flow cytometry results showing the percentage of living CEM cells with (A) no treatment and treatment with (B) RAW264.7 cells, (C) RAW264.7 cells and CpG NFs, (D) RAW264.7 cells and control NFs, or (E) RAW264.7 cells and free CpG for 20 h (bottom-left quadrant of each image showing the percentage of living cells). (F) Time-dependent curve showing the therapeutic efficacy of CpG NFs.

with other delivery approaches, we employed cholesterol-modified CpG, as well as free CpG transfected by lipofect-amine, a widely used commercial transfection agent. The secretion levels of cytokines were then evaluated via an ELISA assay.

We first tested the secretion of TNF-α and IL-6, the cytokines most commonly secreted upon TLR9 activation. The incubation time of CpG NFs and macrophage cells was first optimized (Figure S4), and a period of 8 h was chosen for the following study. After incubation of macrophages with both 100 and 20 nM of each regime for 8 h, the supernatant was collected and centrifuged, followed by ELISA assay to determine the cytokine levels. The ELISA results (Figure 4A) showed that CpG NFs induced dramatic secretion of TNF-α, at levels comparable to those induced by CpG delivered by cholesterol, an approach that has been shown to efficiently penetrate the cell membrane and enter cells and has been reported to be an effective CpG ODN delivery method.[14−16] More impressively, the TNF-α secretion level was significantly higher than that induced by treatment with free CpG or free CpG-transfected lipofectamine. Notably, the control NF showed some degree of stimulation at high concentration. To determine the safe dose range, a concentration-dependent investigation was performed by treating RAW264.7 cells with a series of concentrations of NFs (both CpG and control NFs) and evaluating the secretion level of TNF-α (Figure S5). When the concentration decreased to 10 nM, the stimulation induced by control NFs became negligible, while the stimulation level

from the CpG NF treatment remained high, which is a sign of saturation. Similarly, ELISA assay indicated potent stimulation that resulted in IL-6 secretion (Figure 4B). Here, CpG NFs outperformed all of the other groups, including CpG delivered by conjugation with cholesterol. In addition to TNF-α and IL-6, IL-10 was also tested using ELISA. IL-10, which is usually secreted later than proinflammatory cytokines TNF-α and IL-6 upon immunostimulation, is capable of downregulating the immunostimulatory effect and enhancing the antiinflammatory properties.[28,29] The incubation time for this test was also optimized, and a 24 h period was chosen to perform the experiment (Figure S4). The ELISA results (Figure 4C) indicated that macrophages treated with CpG NFs had a much higher stimulatory effect compared to other groups. It is worth pointing out that the copies of CpG in the NFs may not have been totally released or fully exposed to interact with TLR9, given the spherical structure of NFs. Because currently there have been no methods to determine the number of CpG copies on the surface of NFs, these comparisons are not valid and underestimate the efficacy of CpG NFs. We thus expect that a long-lasting immunostimulatory effect can be achieved because of the resistance of CpG NFs to nuclease digestion, although prior to that, the function of antiinflammatory cytokine IL-10 has to be blocked.[28]

All of the above results have demonstrated the immunostimulatory effects of these NFs incorporated with nucleic acid therapeutic motifs. To further prove that these effects resulted from the specific interaction between CpG motifs and TLR9,

chloroquine, a widely used TLR9 inhibitor,[30] was employed in a blocking study. Particularly, the secretion levels of TNF-α and IL-6 were compared between groups with and without chloroquine treatment. As shown in Figure 4D and E, in the presence of chloroquine, the stimulatory levels of both cytokines were decreased, confirming that TLR9 performed its known biological role in macrophages. Although some TNF-α secretion was observed, this might be attributed to mediation by receptors other than TLR9 or incomplete inhibition of chloroquine on TLR9. Additional confocal imaging displayed that altered uptake of CpG motifs by macrophage cells could be the determining factor in the implementation of immunostimulation (Figure 3). It proved our assumption that the NF-mediated internalization could facilitate the interaction between CpG motifs and TLR9 on endosome surfaces, which showed the strength of the CpG NF as an immunostimulation nanoagent.

To determine the efficacy of CpG NFs as nanoimmunostimulators in the treatment of cancer, we performed a preliminary study to evaluate the inhibitory effects of CpG NFs on the proliferation of in vitro cancer cells. On the basis of the hypothesis that elevated immune cytokines secreted by stimulated immune cells would inhibit cancer cell proliferation, CCRF-CEM cells (T lymphoblast leukemia, suspension cells) were cocultured with RAW264.7 macrophages. At the same time, the coculture system was treated with CpG NFs or other control regimens. Next, supernatants containing CCRF-CEM cells were collected at 4 h intervals during 8−20 h after treatment. The collected supernatant was stained with propidium iodide and FITC−annexin and analyzed using flow cytometry to evaluate the cell viability at each time point. As shown in Figure 5A−E, CCRF-CEM cells treated with CpG NF showed a significantly lower percentage of living cells compared to that of the nontreatment group or the groups treated with either the control NF or free CpG. Furthermore, the inhibition effect elevated as the treatment time increased, as indicated by the decreasing percentage of living cells over time (Figures 5F and S6). These results provide preliminary evidence that our NFs incorporated with CpG nucleic acid therapeutic motifs had therapeutic efficacy.

3. CONCLUSION

In summary, based on the NF platform, we have successfully developed DNA immuno-NFs incorporated with nucleic acid immunostimulatory motif CpG ODNs, which serve as delivery vehicles to efficiently protect and deliver the incorporated nucleic acid therapeutics into immune cells. Considering their favorable properties, these CpG NFs have the potential to be used as immunomodulatory regimens in disease therapy as well as disease prevention.

■ ASSOCIATED CONTENT

Ⓢ Supporting Information

The Supporting Information is available free of charge on the ACS Publications website at DOI: 10.1021/acsami.5b06987.

> Gel electrophoresis characterization of CpG NFs, MTS assay on the biocompatibility of CpG NFs, more confocal images demonstrating the internalization of CpG NFs, time course experiment of CpG NF immunostimulation, expanded data of the therapeutic effect study, DNA sequences used in the study, and

experimental details including materials and methods (PDF)

■ AUTHOR INFORMATION

Corresponding Author
*E-mail: tan@chem.ufl.edu.

Author Contributions
§These authors contributed equally.

Notes
The authors declare no competing financial interest.

■ REFERENCES

(1) Palucka, K.; Banchereau, J. Cancer Immunotherapy via Dendritic Cells. *Nat. Rev. Cancer* **2012**, *12*, 265−277.

(2) Tran, E.; Turcotte, S.; Gros, A.; Robbins, P. F.; Lu, Y. C.; Dudley, M. E.; Wunderlich, J. R.; Somerville, R. P.; Hogan, K.; Hin-richs, C. S.; Parkhurst, M. R.; Yang, J. C.; Rosenberg, S. A. Cancer Immunotherapy Based on Mutation-Specific CD4+ T Cells in a Patient with Epithelial Cancer. *Science* **2014**, *344*, 641−645.

(3) Christ, A.; Temmerman, L.; Legein, B.; Daemen, M. J.; Biessen, E. A. Dendritic Cells in Cardiovascular Diseases Epiphenomenon, Contributor, or Therapeutic Opportunity. *Circulation* **2013**, *128*, 2603−2613.

(4) Mathias, L. J.; Khong, S. M.; Spyroglou, L.; Payne, N. L.; Siatskas, C.; Thorburn, A. N.; Boyd, R. L.; Heng, T. S. Alveolar Macrophages Are Critical for the Inhibition of Allergic Asthma by Mesenchymal Stromal Cells. *J. Immunol.* **2013**, *191*, 5914−5924.

(5) Kobiyama, K.; Aoshi, T.; Narita, H.; Kuroda, E.; Hayashi, M.; Tetsutani, K.; Koyama, S.; Mochizuki, S.; Sakurai, K.; Katakai, Y.; Yasutomi, Y.; Saijo, S.; Iwakura, Y.; Akira, S.; Coban, C.; Ishii, K. J. Nonagonistic Dectin-1 Ligand Transforms CpG into a Multitask Nanoparticulate TLR9 Agonist. *Proc. Natl. Acad. Sci. U. S. A.* **2014**, *111*, 3086−3091.

(6) Teng, X.; Hu, Z.; Wei, X.; Wang, Z.; Guan, T.; Liu, N.; Liu, X.; Ye, N.; Deng, G.; Luo, C.; Huang, N.; Sun, C.; Xu, M.; Zhou, X.; Deng, H.; Edwards, C. K., 3rd; Chen, X.; Wang, X.; Cui, K.; Wei, Y.; Li, J. IL-37 Ameliorates the Inflammatory Process in Psoriasis by Suppressing Proinflammatory Cytokine Production. *J. Immunol.* **2014**, *192*, 1815−1823.

(7) Forte, G.; Rega, A.; Morello, S.; Luciano, A.; Arra, C.; Pinto, A.; Sorrentino, R. Polyinosinic-Polycytidylic Acid Limits Tumor Outgrowth in a Mouse Model of Metastatic Lung Cancer. *J. Immunol.* **2012**, *188*, 5357−5364.

(8) Kawai, T.; Akira, S. The Role of Pattern-recognition Receptors in Innate Immunity: Update on Toll-like Receptors. *Nat. Immunol.* **2010**, *11*, 373−384.

(9) Krieg, A. M. Therapeutic Potential of Toll-like Receptor 9 Activation. *Nat. Rev. Drug Discovery* **2006**, *5*, 471−484.

(10) Latz, E.; Verma, A.; Visintin, A.; Gong, M.; Sirois, C. M.; Klein, D. C. G.; Monks, B. G.; McKnight, C. J.; Lamphier, M. S.; Duprex, W. P.; Espevik, T.; Golenbock, D. T. Ligand-induced Conformational Changes Allosterically Activate Toll-like Receptor 9. *Nat. Immunol.* **2007**, *8*, 772−779.

(11) Krieg, A. M. Toll-like Receptor 9 (TLR9) Agonists in the Treatment of Cancer. *Oncogene* **2008**, *27*, 161−167.

(12) Mutwiri, G. K.; Nichani, A. K.; Babiuk, S.; Babiuk, L. A. Strategies for Enhancing the Immunostimulatory Effects of CpG Oligodeoxynucleotides. *J. Controlled Release* **2004**, *97*, 1−17.

(13) Sands, H.; Gorey-Feret, L. J.; Cocuzza, A. J.; Hobbs, F. W.; Chidester, D.; Trainor, G. L. Biodistribution and Metabolism of

Internally 3H-labeled Oligonucleotides. I. Comparison of a Phosphodiester and a Phosphorothioate. *Mol. Pharmacol.* **1994**, *45*, 932−943.

(14) Liu, H.; Kwong, B.; Irvine, D. J. Membrane Anchored Immunostimulatory Oligonucleotides for In Vivo Cell Modification and Localized Immunotherapy. *Angew. Chem., Int. Ed.* **2011**, *50*, 7052−7055.

(15) Liu, H.; Moynihan, K. D.; Zheng, Y.; Szeto, G. L.; Li, A. V.; Huang, B.; Van Egeren, D. S.; Park, C.; Irvine, D. J. Structure-based Programming of Lymph-node Targeting in Molecular Vaccines. *Nature* **2014**, *507*, 519−522.

(16) Rattanakiat, S.; Nishikawa, M.; Takakura, Y. Self-assembling CpG DNA Nanoparticles for Efficient Antigen Delivery and Immunostimulation. *Eur. J. Pharm. Sci.* **2012**, *47*, 352−358.

(17) Dalpke, A. H.; Zimmermann, S.; Albrecht, I.; Heeg, K. Phosphodiester CpG Oligonucleotides as Adjuvants: Polyguanosine Runs Enhance Cellular Uptake and Improve Immunostimulative Activity of Phosphodiester CpG Oligonucleotides In Vitro and In Vivo. *Immunology* **2002**, *106*, 102−112.

(18) Wei, M.; Chen, N.; Li, J.; Yin, M.; Liang, L.; He, Y.; Song, H.; Fan, C.; Huang, Q. Polyvalent Immunostimulatory Nanoagents with Self-assembled CpG Oligonucleotide-conjugated Gold Nanoparticles. *Angew. Chem., Int. Ed.* **2012**, *51*, 1202−1206.

(19) Lin, A. Y.; Mattos Almeida, J. P.; Bear, A.; Liu, N.; Luo, L.; Foster, A. E.; Drezek, R. A. Gold Nanoparticle Delivery of Modified CpG Stimulates Macrophages and Inhibits Tumor Growth for Enhanced Immunotherapy. *PLoS One* **2013**, *8*, e63550.

(20) Chen, N.; Wei, M.; Sun, Y.; Li, F.; Pei, H.; Li, X.; Su, S.; He, Y.; Wang, L.; Shi, J.; Fan, C.; Huang, Q. Self-Assembly of Poly-Adenine-Tailed CpG Oligonucleotide-Gold Nanoparticle Nanoconjugates with Immunostimulatory Activity. *Small* **2014**, *10*, 368−375.

(21) Li, J.; Pei, H.; Zhu, B.; Liang, L.; Wei, M.; He, Y.; Chen, N.; Li, D.; Huang, Q.; Fan, C. Self-Assembled Multivalent DNA Nanostructures for Noninvasive Intracellular Delivery of Immunostimulatory CpG Oligonucleotides. *ACS Nano* **2011**, *5*, 8783−8789.

(22) Nishikawa, M.; Ogawa, K.; Umeki, Y.; Mohri, K.; Kawasaki, Y.; Watanabe, H.; Takahashi, N.; Kusuki, E.; Takahashi, R.; Takahashi, Y.; Takakura, Y. Injectable, Self-gelling, Biodegradable, and Immunomodulatory DNA Hydrogel for Antigen Delivery. *J. Controlled Release* **2014**, *180*, 25−32.

(23) Klinman, D. M. Immunotherapeutic Uses of CpG Oligodeoxynucleotides. *Nat. Rev. Immunol.* **2004**, *4*, 249−258.

(24) Zhu, G.; Hu, R.; Zhao, Z.; Chen, Z.; Zhang, X.; Tan, W. Noncanonical Self-Assembly of Multifunctional DNA Nanoflowers for Biomedical Applications. *J. Am. Chem. Soc.* **2013**, *135*, 16438−16455.

(25) Hu, R.; Zhang, X.; Zhao, Z.; Zhu, G.; Chen, T.; Fu, T.; Tan, W. DNA Nanoflowers for Multiplexed Cellular Imaging and Traceable Targeted Drug Delivery. *Angew. Chem., Int. Ed.* **2014**, *53*, 5821−5826.

(26) Shopsowitz, K. E.; Roh, Y. H.; Deng, Z. J.; Morton, S. W.; Hammond, P. T. RNAi-Microsponges Form through Self-Assembly of the Organic and Inorganic Products of Transcription. *Small* **2014**, *10*, 1623−1633.

(27) Singh, A.; Talekar, M.; Raikar, A.; Amiji, M. Macrophage-targeted Delivery Systems for Nucleic Acid Therapy of Inflammatory Diseases. *J. Controlled Release* **2014**, *190*, 515−530.

(28) Duramad, O.; Fearon, K. L.; Chan, J. H.; Kanzler, H.; Mar-shall, J. D.; Coffman, R. L.; Barrat, F. J. IL-10 Regulates Plasmacytoid Dendritic Cell Response to CpG-containing Immunostimulatory Sequences. *Blood* **2003**, *102*, 4487−4492.

(29) Vicari, A. P.; Chiodoni, C.; Vaure, C.; Ait-Yahia, S.; Der-camp, C.; Matsos, F.; Reynard, O.; Taverne, C.; Merle, P.; Colombo, M. P.; O'Garra, A.; Trinchieri, G.; Caux, C. Reversal of Tumor-induced Dendritic Cell Paralysis by CpG Immunostimulatory Oligonucleotide and Anti−Interleukin 10 Receptor Antibody. *J. Exp. Med.* **2002**, *196*, 541−549.

(30) Kuznik, A.; Bencina, M.; Svajger, U.; Jeras, M.; Rozman, B.; Jerala, R. Mechanism of Endosomal TLR Inhibition by Antimalarial Drugs and Imidazoquinolines. *J. Immunol.* **2011**, *186*, 4794−4804.